IEEE Open Journal of Vehicular Technology

Received 17 January 2020; accepted 1 March 2020. Date of publication 10 March 2020;
date of current version 8 April 2020. The review of this paper was arranged by Editor P. H. J. Chong.

Digital Object Identifier 10.1109/OJVT.2020.2979820

QoS-Aware Capacity Planning of Networked PEV Charging Infrastructure

AHMED ABDALRAHMAN (Student Member, IEEE) AND WEIHUA ZHUANG (Fellow, IEEE)

Department of Electrical and Computer Engineering, University of Waterloo, Waterloo, ON N2L 3G1, Canada

CORRESPONDING AUTHOR: A. ABDALRAHMAN (e-mail: aabdalra@uwaterloo.ca)

This work was supported by a research grant from the Natural Sciences and Engineering Research Council (NSERC) of Canada.

ABSTRACT Plug-in electric vehicle (PEV) charging infrastructure is necessary to accommodate the rapid increase in PEV penetration rate. Capacity planning of PEV charging infrastructure (EVCI) must ensure not only a satisfactory charging service for PEV users but also a reliable operation of the power grid. In this paper, we propose a quality-of-service (QoS) aware capacity planning of EVCI. In particular, the proposed framework accounts for the link between the charging QoS and the power distribution network (PDN) capability. Towards this end, we firstly optimize charging facility sizes to achieve a targeted QoS level. Then, we minimize the integration cost for the PDN by attaining the most cost-effective allocation of the energy storage systems (ESSs) and/or upgrading the PDN substation and feeders. Additionally, we capture the correlation between the occupation levels of neighboring charging facilities and the blocked PEV user behaviors. We model the EVCI as a queuing network with finite capacity, and utilize the non-stationary queuing models to study the temporal variability of the PEV charging demand. A network of charging facilities is used to demonstrate the effectiveness of the proposed framework.

INDEX TERMS Capacity planning, charging infrastructure, distribution network, energy storage system, non-stationary queues, queueing networks.

NOMENCLATURE

Indices and Sets

T	Set of time segments over a day, indexed by t.
N	Set of all facilities in EVCI, indexed by n.
$\mathcal{B}$	Set of all PDN buses, indexed by j.
$\mathcal{L}$	Set of all PDN branches, indexed by ij.
S	Set of all load scenarios, indexed by s.

Parameters

$\mathcal{P}$	PEV penetration rate.
ν	Average charging frequency of a PEV.
Θ^{τ}	Targeted throughput [%].
W^{τ}	Targeted expected waiting time [minutes].
C^{P}	Cost of ESS power rating [$/kW].
C^{E}	Cost of ESS energy rating [$/kWh].
C^{Sb}	Cost of substation expanding [$/kVA].
C^{F}	Cost of feeder upgrading [$/kVA.km].
O_l^C	Annual ESS operational cost at year l [$/kWh/year].
L	ESS life time [years].
$\mathcal{I}$	Annual interest rate [%].
ℓ_{ij}	Feeder length [km].
$C_{s,t}^{e}$	Day-ahead hourly energy cost at load scenario s time t [$/kWh].
η^{ES}	ESS charging/discharging efficiency [%].
$\triangle t$	Time segment duration.
$v_{\min}$, $v_{\max}$	Minimum and maximum bus voltage [p.u].

Variables

$\lambda_{t,n}^{*}$	Modified offered load arrival rate to facility n at time t.
c_n, B_n	Number of chargers/waiting positions allocated in facility n.
$p_{i_{t,n}}$	Probability of having i PEVs in facility n at time t.
P_n^R, E_n^R	Rated power/energy capacity of ESS at facility n [kW], [kWh].
G_j^R	Rated expansion power of substation connected to bus j [kVA].
S_{ij}^R	Rated upgrade power of the feeder connecting buses i and j [kVA].

$P^{ES}_{s,t,n}$	ESS charging/discharging power at facility n at load scenario s at time t [kW].
$E_{s,t,n}$	Stored energy in ESS at facility n at load scenario s at time t [kWh].
$P^{EV}_{t,n}$	Power demand of charging facility n at time t [kW].
$P^{G}_{s,t,j}$, $Q^{G}_{s,t,j}$	Active/reactive power provided by substation at bus j at load scenario s at time t [MW], [MVAr].
$P^{D}_{s,t,j}$, $Q^{D}_{s,t,j}$	Active/reactive load demand at bus j at load scenario s at time t [MW], [MVAr].
$P_{s,t,ij}$, $Q_{s,t,ij}$	Active/reactive power flow at branch connecting buses i and j at load scenario s at time t [MW], [MVAr].
$L_{s,t,ij}$	Squared current magnitude of branch connecting buses i and j at load scenario s at time t [p.u].
$V_{s,t,j}$	Squared voltage magnitude of bus j at load scenario s at time t [p.u].
p_n	Variable controls ESS power rating at facility n.
e_n	Variable controls ESS energy capacity at facility n.
g_j	Variable controls the expansion of substation connected to bus j.
f_{ij}	Variable controls the capacity upgrade of feeder connecting buses i and j.

I. INTRODUCTION

The number of plug-in electric vehicles (PEVs) is rapidly increasing worldwide, because of the increased social awareness of their environmental and economic benefits [1]. A PEV charging infrastructure (EVCI), which consist of various types of public charging facilities, is necessary to accommodate the increasing PEV charging demand [2]. Capacity planning of EVCI is a problem of determining appropriate sizes for charging facilities that quantify the number of chargers and waiting positions. Capacity planning of EVCI must deal with both the PEV user requirements and the service providers utility. From the PEV user perspective, charging facilities should be appropriately sized to prevent service congestion and fulfill the stochastic and time-varying charging demand. From the service provider perspective, capacity planning of EVCI must minimize the investment cost associated with charging facility construction and integration with the PDN by optimizing the numbers of chargers and waiting positions allocated at each charging facility, and ensuring that the load demand of EVCI complies with power grid constraints. Charging quality-of-service (QoS) is a measure of PEV user satisfaction. Although increasing the facility sizes enhances the charging QoS, it presents a substantial load to the power grid that may exceed the capability of power distribution network (PDN). To accommodate the expected power demand of charging facilities, PDN components (i.e., feeders and substations) may need upgrade, which in turn requires huge investments. Utilizing an energy storage system (ESS) in charging facilities can be a solution to alleviate the required PDN upgrades if the ESS cost is less than the reinforcements cost [3]. Consequently, there are inter-relationships among the QoS level of EVCI, the required PDN upgrades, and the ESS allocation in charging facilities. These inter-relationships offer guidance to size the charging facilities in a cost-effective manner, in addition to provide insights into how to make a trade-off between the PEV user satisfaction and the required investment in PDN.

Existing capacity planning models of EVCI follow two main approaches [1]. One approach uses stochastic models to size the charging facilities to achieve a targeted QoS level [2], [4]. A charging facility is modeled as an isolated stationary queue, while PEVs are modeled as customers in the queue. These PEVs require a charging service from a limited number of identical chargers. Charging facilities are sized based on the expected PEV charging demand at each facility location and evaluated based on statistical metrics, such as blocking probability and waiting time [4]. The $M/M/c$ queuing model can be used to model fast charging stations [4]–[7]. This model assumes that all the arrived PEVs will wait for the charging service, which means unlimited waiting positions in the charging facility. In order to consider the limited waiting positions in a charging station, the $M/M/c/K$ queuing model is employed [8], [9]. If all the waiting positions in the facility are occupied, the newly arrived PEV will leave the facility without charging. Based on the expected PEV charging demand, the numbers of chargers and waiting positions in the charging facility can be determined to meet the target QoS set by the planner [4], [8], [9]. Although this approach can ensure a satisfactory charging service with the stochastic PEV demand, it endangers the reliability of the power system. This is because the targeted QoS level is set in isolation from the actual capability of PDN.

The other approach sizes the charging facilities to minimize the negative impacts on the power grid [10]–[12]. The sizing objective is to ensure that the charging facility load demand complies with the power system operational constraints by collaboratively planning the EVCI and PDN. For instance, a multi-objective planning model with a coupled distribution and transportation networks is proposed in [13]. The planning model optimizes the locations and sizes of charging facilities to minimize the total energy loss and bus voltage deviation on the distribution network, in addition to maximizing the captured traffic flow of charging facilities. Another model is to optimize the locations and sizes of charging facilities to balance between the PEV charging requirement and power network stability, considering a linearized power network model [14]. This approach ensures that the PDN can safely accommodate the peak load demand of charging facilities; however, PEV user satisfaction is not a focus. This is because the planning models usually re-locate and/or re-size the charging facilities to fulfill power grid requirements.

There are a few published papers that deal with both the charging QoS and the PDN capability in the planning of EVCI. For instance, a siting and sizing model of fast charging stations on coupled transportation and power networks is

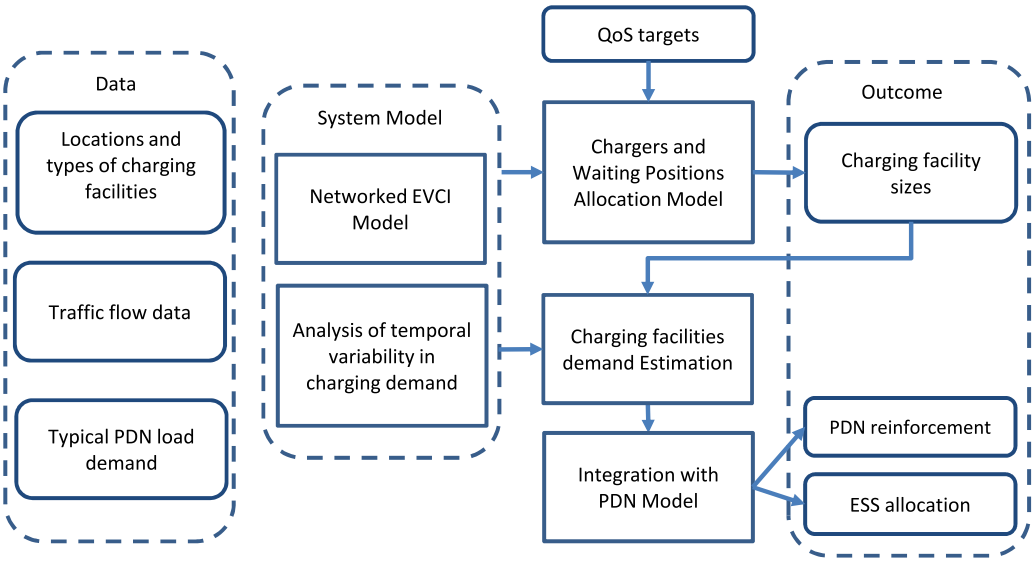

FIGURE 1. EVCI capacity planning Framework.

proposed in [15]. This model utilizes users' waiting time at charging facilities as a service level index. Then, an optimization model is used to size charging stations and determine the required upgrade in the PDN. In [6], a capacitated flow-refueling location model is proposed to optimize the planning of highway fast-charging stations. The proposed model adopts the $M/G/S$ queuing model to size charging facilities based on the upper limit of users' waiting time. This model also introduces capacity constraints in the siting model. Thereby, if PEV charging demand cannot be satisfied in a facility, it is distributed to other facilities in the network.

Even though that capacity planning of EVCI has been extensively studied in the literature, three issues have not yet been well studied: 1) Existing capacity planning models do not capture the inter-relationships among the charging QoS, the capability of existing PDN, and the possibility of allocating ESS in charging facilities. Accounting this relationship in the sizing of charging facility ensures the balance between the requirements of the power system and charging service; 2) Modeling charging facilities as isolated queues with infinite capacity ignores the correlation among the occupation levels of nearby facilities. In practice, if the capacity of a charging facility is less than the demand, the blocked PEV users can spread across the surrounding charging facilities, which can greatly impact the level of performance in those facilities. Therefore, charging facilities must be modeled as a network with a finite capacity to account for the inter-relationships among nearby facilities, in addition to accounting for the behavior of blocked PEV users by the overloaded facilities; 3) Designing charging facilities using the stationary queueing models do not account the temporal variability of PEV charging demand. Two approaches are used to apply these stationary queuing models to a system with time-varying demand (PEV arrival rate). The first approach uses stationary models with the long-run-average arrival rate to simplify the sizing problem [4]. However, the system can suffer from high congestion (overload) and low QoS at the peak demands [16]. The second approach divides the time horizon into intervals and then uses the peak demand (peak arrival rate) as inputs to the stationary queuing models [2], [11]. This approach aims to fulfill the targeted performance at the peak demand. However, it fails to capture the random time lag between the time of peak demand and the time of peak load on the queuing system. Moreover, this approach does not account for PEVs that are already in the system (either charging or waiting) from the preceding time periods [16].

Different from the existing studies, in this paper, we present a QoS-aware capacity planning framework of networked EVCI. The major contributions of this study are as follows:

1) The new capacity planning framework takes account of the inter-relationships among the targeted QoS, ESS allocation, and PDN upgrade. As illustrated in Fig. 1, the proposed framework consists of two models that are solved sequentially: Firstly, the capacity planning of EVCI model is used to optimize the numbers of chargers and waiting positions allocated at each charging facility to realize the targeted QoS level for the entire networked EVCI. After that, PEV charging demand at each facility is estimated for inclusion in the PDN load demand. Finally, the integration with the PDN model is used to minimize the integration cost of EVCI with PDN by attaining the most cost-effective ESS allocation and/or PDN reinforcement;
2) The proposed EVCI model captures the correlation among the occupation levels of neighboring charging facilities, in addition to blocked PEV user behaviors. Towards this end, we model the EVCI as an open queuing network with finite capacity and blocking;

3) The proposed approach accounts for the temporal variability of the charging demand by modeling the charging facilities as non-stationary queue systems. Then, a modified arrival rate function is derived to approximate the steady state performance of the systems.

The rest of this paper is organized as follows. Section II presents the system model, along with an illustration of modeling the EVCI as a queuing network and accounting for the temporal variability of charging demand. Section III describes the proposed capacity planning model for EVCI. Section IV discusses the integration model with PDN. Numerical results are given in Section V to evaluate the proposed planning framework. Finally, conclusions are drawn in Section VI.

II. SYSTEM MODEL

Consider a typical urban area where the road transportation network (RTN) is coupled with the PDN according to the geographical information. The RTN consists of a finite set of nodes (e.g., road intersections and highway exits) and a finite set of directed links (e.g., streets and traffic lanes) connecting any two nodes in the network. The PDN consist of a set of buses $\mathcal{B}$ and a set of branches (feeders) $\mathcal{L}$. The PDN is connected to the rest of the power grid through substation(s). Let $\mathcal{H}$ ($\mathcal{H} \subset \mathcal{B}$) be the set of buses connected to substations. It is assumed that load forecasting studies are conducted at the PDN to estimate the power demand profile [11]. Furthermore, voltage limits, branch capacity limits, substation capacity limits, and the conductance of all branches are known. Time is partitioned to equal segments, where T denotes the set of all time segments over a 24-hour time horizon and is indexed by t. Each time segment duration is chosen to be one hour as an example. This is because energy trading and scheduling are conducted on a one-hour interval basis, according to Ontario's independent electricity system operator (IESO) [17]. Also, PEV traffic flows are estimated on the same time intervals.

The EVCI consists of three types of public charging facilities, which are parking lots (PLs) with AC chargers, DC fast charging stations (FCSs), and on-road wireless chargers (OWCs) [2], [18]. The OWC is a relatively new charging technology that enables PEV to dynamically charging while driving on dedicated charging lanes through wireless power transfer technology [19]. The set of all charging facilities in the EVCI is denoted as N, which is composed of three subsets: subset W for OWCs, subset F for FCSs, and subset P for PLs, where $|W \cup F \cup P| = |N|$. The locations of charging facilities are given. FCSs and PLs are allocated on a finite set of RTN nodes, and OWCs are allocated on a finite set of RTN links. AC level 3 chargers and DC fast chargers are deployed in the PLs and FCSs, respectively [18]. Moreover, some PEVs are capable of charging in OWCs via the dedicated wireless charging lanes [2]. Hence, a PEV may step into this charging lane to get a charging service, then return back to the normal traffic after charging. The load demand of charging facility equals the aggregated charging demand of all PEVs simultaneously being charged.

A. NETWORKED EVCI MODEL

The capacity of any charging facility is always finite. Thereby, a PEV user may be momentarily stopped (rejected) when a charging facility reaches its maximum capacity. This phenomenon is called blocking. Subsequently, the blocked PEV user may move towards one of the neighboring charging facilities, requesting a charging service. Due to the blocking, there is a correlation among the PEV occupancy of neighboring charging facilities, and understanding this correlation helps to explain the propagation of congestion. Consequently, a realistic model of EVCI should address the finite capacity of charging stations, in addition to the behavior of blocked PEV users by the overloaded facilities.

EVCI can be modeled as an open queuing network with finite capacity and blocking. Different from isolated queue models, a finite capacity queuing network can capture the interactions among multiple charging facilities, in addition to the blocked PEV user behaviors. In such a network, EVCI can be represented as a set of interconnected charging facilities (service centers). These service centers are interconnected through a road system. PEV users enter this open network from outside (exogenous arrivals), receive charging services, and eventually leave the network. In order to construct the queuing network, each charging facility is modeled by two types of nodes:

- *Charging facility node (CN):* A charging facility is represented as a physical node. If the charging facility is an FCS or a PL, CN n ($n \in N$) can be modelled as a finite queuing system $M/M/c_n/K_n$, which has a Poisson arrival process M [20], exponentially distributed service time M with service rate μ_n [7], c_n chargers (servers), and maximum number of PEVs, K_n, in the facility including the charging and waiting PEVs. If the charging facility is an OWC, CN node n can be represented as a loss system $M/M/c_n/c_n$, since there is no waiting position on the charging lanes.
- *Decision-making node (DN):* A DN is a logical (virtual) node associated with each CN. DN n is used to model the behavior of PEV users, who are requesting a charging service from the associated CN. The decision of each PEV user can be either to get a charging service from CN n or move towards another charging facility (DN $\acute{n}$, where $\acute{n} \neq n$). Thus, the arrivals to a DN can be from an external population and/or routed from other DNs. DN n is modeled as a single server queue $M/M/1$ with a very high service rate $\mu_n^d \gg \mu_n$ since a driver usually makes a decision instantaneously without delay.

In the networked EVCI, PEV user behaviors in response to the occupancy level of charging facilities are described through a blocking mechanism, called *repetitive service with random destination (RS-RD)* [21]. When a PEV user chooses charging facility n for a service, the user will first arrive at DN n, then chooses a destination randomly either by attempting to access CN n or routing towards another DN $\acute{n}$ in the network. If CN n at that time is full, the user will be blocked and

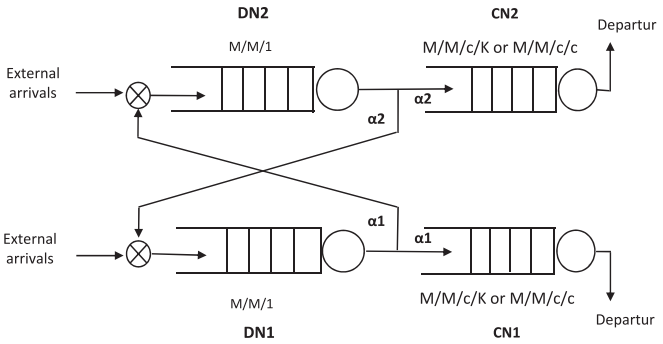

FIGURE 2. Queuing network model of two neighboring facilities.

return to DN n, starting to randomly choose a new destination independent of the previous choice(s).[1] After a PEV is served by a charging facility, it leaves the network with probability 1, under the assumption that the charging demand of a PEV is unsplittable and a PEV will be charged with sufficient energy at the visited facility. An illustrative example of a queuing network composing of two neighboring charging facilities is shown in Fig. 2.

The routing probability between two charging facilities is denoted by $\alpha_{n\acute{n}}$, where $n \neq \acute{n}$ and $n, \acute{n} \in N$, while α_{nn} denotes the routing probability between DN n and the associated CN n. The routing probability α_{nn} is larger than any $\alpha_{n\acute{n}}$, for $\acute{n} \neq n$, where $\alpha_{n\acute{n}}$ are assigned to the neighboring DNs depending on the proximity to CN n. That is, a blocked PEV will be routed to a nearby charging facility with a higher probability than those to farther facilities. This assumption conforms with vehicular traffic modeling [23]. The routing probability can be estimated based on the multinomial logit (MNL) model, which is used to predict driver choice probabilities as a function of a certain utility, such as traveling distance, traveling time, and charging cost [24]. Due to the range anxiety of the blocked PEV users, $\alpha_{n\acute{n}}$ is assumed depending on the distance $d_{n\acute{n}}$ between charging facilities and can be estimated by

$$1 - \alpha_{nn} = \sum_{\substack{\forall i \in N \\ i \neq n}} \alpha_{ni}, \tag{1a}$$

$$\alpha_{n\acute{n}} = \frac{(1 - \alpha_{nn}) e^{-d_{n\acute{n}}}}{\sum_{\substack{\forall i \in N \\ i \neq n}} e^{-d_{ni}}}, \quad \forall n \in N. \tag{1b}$$

Analysis of queuing networks with finite capacity and blocking is complex, because the steady-state queue length distributions do not have a product form, except for some special cases [21]. However, the steady-state queue length distribution of the network under investigation can be approximated using the disaggregation-aggregation (DA) iteration method [25]. Based on DA iterations, the underlying Markov chain model of a queuing network is approximated through aggregation. This Markov chain typically has a very large state space and a sparse transition probability matrix. DA iterations exploit the marginal aggregate probabilities instead of the complete state space, in order to approximate a product form solution of the state probabilities. Calculating the state probabilities facilitates the evaluation of the performance indicators of the EVCI.

[1] A deadlock problem may occur in the queuing network if all CNs in the network are full. In this case, a PEV user may be blocked multiple times until space becomes available at a CN. To avoid a network deadlock, it is sufficient that the routing matrix is irreducible and the number of PEVs requesting charging services is less than the total capacity of CNs [22] In this model, we assumed that the EVCI is a deadlock-free network.

B. ANALYSIS OF TEMPORAL VARIABILITY IN CHARGING DEMAND

To incorporate the time-varying demand, a charging facility model can be refined using non-stationary queuing models $M_t/M/c/K$ and $M_t/M/c/c$ (depending on the facility type) with a non-homogeneous Poisson arrival process (NHPP) M_t. The NHPP is a counting process, $\boldsymbol{\mathcal{N}} = \{\mathcal{N}(t) : t \geq 0\}$, having independent and Poisson-distributed increments. The NHPP has a deterministic arrival rate function at time t, $\lambda(t)$, [26].

The analysis of non-stationary queuing models can be approximated by infinite server model $M_t/M/\infty$, which has the same arrival process and service time distribution but with an infinite number of servers [27]. This approximation allows all users to access the service upon arrival without waiting, which simplifies the mathematical model. The PEV number, $\mathcal{N}_t$ at time t, in the finite queuing model is approximated by the number of the busy servers, $\mathcal{N}_t^{\infty}$, in the infinite server model. It is proved, in [27] and the references therein, that $\mathcal{N}_t^{\infty}$ has a Poisson distribution with mean, $m_{\infty}(t)$, which is expressed in terms of the arrival-rate function $\lambda(t)$ as

$$m_{\infty}(t) \equiv E[\mathcal{N}_t^{\infty}] = E\left[\int_{t-\mathbb{S}}^{t} \lambda(r) dr\right] = E[\lambda(t - \mathbb{S}_e)] \cdot E[\mathbb{S}] \tag{2}$$

with $\mathbb{S}$ being the service time distribution. In (2), random variable $\mathbb{S}_e$ is the stationary-excess distribution, which indicates the distribution of the remaining service time [28]. The time-varying mean in (2) is the expected number of busy servers in the system with an infinite number of servers, referred to as *offered load*. This formula is complicated as there is a random time lag, $\mathbb{S}_e$, in the arrival rate function. The offered load of infinite server model provides insight on both the time-lag and magnitude shift between arrivals and loads of the system.

The offered load approximation in (2) is used to derive a new arrival rate function, which is used in evaluating the performance of the non-stationary queuing systems over time. The new arrival rate function is called *modified offered load (MOL)* [16], [28]. Based on the MOL, the instantaneous performance measures for the $M_t/M/c/K$ and $M_t/M/c/c$ systems can be approximated with the steady state performance of the associated stationary models $M/M/c/K$ and $M/M/c/c$, respectively. The MOL arrival rate function, $\lambda^*(t)$, is obtained from the exponentially weighted moving average of the arrival rate for the non-stationary models by [28]

$$\lambda^*(t) = \int_{-\infty}^{t} \mu e^{-\mu(t-u)} \lambda(u) du \tag{3}$$

where μ is the service rate of the queuing model. The MOL arrival rate accounts for the transient behavior and dependencies among the consecutive intervals. Thereby, the time-dependent system performance can be analyzed accurately [16].

The non-parametric estimation method is used to estimate the MOL arrival rate function over time [26]. The MOL arrival rate function to charging facility n, $\lambda^*_{t,n}$, is assumed piecewise constant on any subinterval $[t-1, t)$, with $t \in T$, depending on the number of PEVs intercepted at a charging facility, PEV penetration rate, and the facility type. Let $I^n_1, I^n_2, \ldots, I^n_{|T|}$ be the numbers of PEVs intercepted at charging facility n, which are collected over $|T|$ sub-intervals. These numbers are estimated based on the dynamic traffic assignment model, which forecasts the time-varying traffic patterns of RTN [2]. Thus, MOL arrival rate function for charging facility n at time slot t can be calculated by

$$\lambda^*_{t,n} = \begin{cases} \mathcal{P}\nu(1-\sigma)(1-\beta)\int_{u=0}^{t} \mu^F e^{-\mu^F(t-u)} I^n_u du, & \text{if } n \in F \\ \mathcal{P}\nu(1-\sigma)\beta\int_{u=0}^{t} \mu^W e^{-\mu^W(t-u)} I^n_u du, & \text{if } n \in W \\ \mathcal{P}\nu\sigma\int_{u=0}^{t} \mu^P e^{-\mu^P(t-u)} I^n_u du, & \text{if } n \in P \end{cases} \tag{4}$$

where $\mathcal{P}$ represents the PEV penetration rate; ν is the average charging frequency of a PEV; σ denotes the percentage of PEV drivers who prefer charging in PLs at trip destinations; β denotes the percentage of PEVs that have wireless charging capability; and μ^F, μ^W, μ^P denote service rates of FCS, OWC, and PL, respectively.

III. CAPACITY PLANNING OF EVCI

This planning stage focuses on developing a capacity planning model for EVCI as a resource provisioning problem without considering limits of the PDN. It resolves the issue of sizing the charging facilities efficiently by optimizing the number of chargers and waiting positions required at charging facilities to achieve the targeted QoS level for EVCI.

The allocation of chargers $\mathbf{c} = \{c_n, \forall n \in N\}$ and waiting positions $\mathbf{B} = \{B_n, \forall n \in N\}$, where $B_n = K_n - c_n$, in charging facilities affects the overall performance of the charging service and hence customer satisfaction. Obviously, the numbers of chargers and waiting positions allocated to a charging facility lead to differences in the facility's operational capacity, and hence the blocking probability and the expected waiting time. Furthermore, with the propagation of congestion (due to the behaviors of the blocked PEV users), the performance of entire networked EVCI may vary in proportional to the sizes of individual facilities. Thereby, the capacity of each charging facility must be optimized to realize the targeted QoS level for the entire networked EVCI, given that both chargers and waiting positions represent a significant amount of investment during the deployment phase. Two performance metrics are used to measure the QoS at the networked EVCI:

1) The normalized network throughput at time t, Θ_t, measures the percentage of PEV users who can get charging services successfully without being blocked. The more blocked PEVs in a charging facility, the less user satisfaction since the blocked users have to go to another facility to get charging services. The throughput can be obtained by

$$\Theta_t(\mathbf{c}, \mathbf{B}) = \frac{\sum_{\forall n \in N} \lambda^*_{t,n}(1 - p_{K_{t,n}})}{\sum_{n \in N} \lambda^*_{t,n}} \tag{5}$$

where $p_{K_{t,n}}$ denotes the blocking probability of charging facility n at time t. Note that Θ_t is a function of the time-varying MOL arrival rate to charging facilities, in addition to the numbers of servers and waiting positions of all facilities in the networked EVCI. The lower bound of the normalized network throughput, $\underline{\Theta}$, is defined as

$$\underline{\Theta}(\mathbf{c}, \mathbf{B}) = \min_{\forall t \in T} \Theta_t * 100\%. \tag{6}$$

2) The expected waiting time, $E[W_{t,n}]$, measures the speed of getting a charging service. As PEV users wait longer, their satisfaction level decreases. The expected waiting time at charging facility n at time t can be obtained by

$$E[W_{t,n}(\mathbf{c}, \mathbf{B})] = \frac{\sum_{i=c_n+1}^{K_n} (i - c_n) p_{i_{t,n}}}{\lambda^*_{t,n}(1 - p_{K_{t,n}})} \tag{7}$$

where $p_{i_{t,n}}$ denotes the probability of having i PEVs in charging facility n at time t. On the entire network level, the weighted average at time t over all charging facilities, W^{Net}_t, and the upper bound, $\overline{W^{Net}}$, of the expected waiting time metric are given by

$$W^{Net}_t(\mathbf{c}, \mathbf{B}) = \frac{1}{|N|} \sum_{\forall n \in N} \omega'_{t,n} E[W_{t,n}] \tag{8a}$$

$$\overline{W^{Net}}(\mathbf{c}, \mathbf{B}) = \max_{t \in T} W^{Net}_t \tag{8b}$$

where $\omega'_{t,n} = \frac{\lambda^*_{t,n}}{\sum_{n \in N} \lambda^*_{t,n}}$ is a weighting factor that accounts for the differences in charging facility demands. It gives more weight to facilities with a higher demand, and vice versa. Again, W^{Net}_t is a function of the MOL arrival rates and the networked EVCI characteristics.

It assumed that PEV users do not have prior knowledge about the current QoS at the chosen facility. Upon arriving at a charging facility, a PEV user spontaneously attempts to access the charging facility to get a charging service. If the charging facility at that time is full, the user will be blocked and choose a new destination. The investigation of how the QoS and charging price affect the PEV user behaviors is left for our future research.

In the sizing problem, both numbers of chargers and waiting positions are minimized to fulfill the given QoS targets for the networked EVCI, which is formulated as

$$\min_{\mathbf{c},\mathbf{B}} \left\{ \sum_{\forall n \in N} \omega_n c_n + \sum_{\forall n \in N} (1 - \omega_n) B_n \right\} \tag{9a}$$

$$\text{s.t. } \underline{\Theta}(\mathbf{c}, \mathbf{B}) \geq \Theta^{\tau} \tag{9b}$$

$$\overline{W^{Net}}(\mathbf{c}, \mathbf{B}) \leq W^{\tau} \tag{9c}$$

$$c_n \in \{1, 2, \ldots\}, \quad \forall n \in N \tag{9d}$$

$$B_n = \begin{cases} \{0, 1, 2, \ldots\}, & \text{if } n \in \{F \cup P\} \\ 0, & \text{if } n \in \{W\}. \end{cases} \tag{9e}$$

The objective function (9a) minimizes the total number of the allocated chargers and waiting positions in the given queuing network. For each charging facility, a relative cost variable, ω_n, is assigned to the chargers and $(1 - \omega_n)$ to the waiting positions. The value of ω_n reflects the relative cost of a charger versus that of a waiting position for each specific charging facility, $n \in N$. Constraint (9b) ensures that $\underline{\Theta}(\mathbf{c}, \mathbf{B})$ is not less than predefined targeted network throughput Θ^{τ}. Constraint (9c) ensures that $\overline{W^{Net}}(\mathbf{c}, \mathbf{B})$ is not larger than predefined maximum expected waiting time threshold W^{τ}. Constraint (9d) forces the number of chargers to be a positive integer. Constraint (9e) forces the number of waiting positions to be a positive integer if the charging facility is an FCS or PL, and to be 0 if the charging facility is an OWC.

The optimization problem simultaneously determines **c** and **B** to satisfy the targeted QoS level. However, establishing appropriate QoS thresholds is not a trivial task. These thresholds are determined based on the actual capability of PDN as described in the next section. The sizing problem in (9) is a difficult nonlinear integer programming (NIP) problem with black-box constraints. Because the analytical expressions of the two performance metrics (i.e., $\underline{\Theta}(\mathbf{c}, \mathbf{B})$ and $\overline{W^{Net}}(\mathbf{c}, \mathbf{B})$) of the networked EVCI are unknown, and exact derivatives cannot be provided for those black-box constraints. The values of these functions can be evaluated only through the expensive (time-consuming) DA iteration algorithm.

It is shown that the optimal allocation of the scarce resources in a network is an $\mathcal{NP}$-hard problem [29]. The number of integer variables in the problem is $2N$, and the solution space of the sizing problem grows exponentially with an increase of the number of the networked charging facilities. Additionally, the evaluation time of the black-box constraints grows exponentially with an increase of both the number of nodes in the network and the capacity of the individual nodes.

The mixed-integer sequential quadratic programming (MISQP) algorithm is chosen to solve the optimization problem. The MISQP is a derivative-free heuristic iterative algorithm that searches for a local minimum solution relaying on information obtained from the evaluation of several points in the search space [30], [31]. This algorithm is used in solving the problems with a relatively small number of variables, in which the integer variables are not relaxable (i.e. the function variables can only evaluated at integer points). The MISQP requires a few number of function evaluations, which is a suitable choice for the expensive black-box constraints in the sizing problem. To increase the chances of finding the global optimal solution, the solution algorithm can be initialized with different random starting solutions.

IV. EVCI INTEGRATION INTO POWER GRID

So far, the sizes of networked EVCI are optimized to satisfy the targeted QoS metrics, but without accounting for the operational and electrical constraints of the existing PDN. The next step is to integrate charging facilities into PDN, which add a substantial load to the power grid. Originally, the existing system components of the PDN may not be designed to accommodate the power demand of charging facilities [32]. To facilitate the integration of charging facilities, PDN substations and feeders may need to be reinforced, which requires new investments. Alternatively, ESSs can be allocated in charging facilities to alleviate the PDN integration cost if using ESS is more cost-effective. When utilizing an ESS, energy is stored during off-peak times and released when the total system load (i.e., system demand in addition to EVCI demand) is high. The charging service provider will benefit from covering PEV charging demand in charging facilities, in addition to energy arbitrage profit if the ESS is used on the system demand. This section presents a planning framework that minimizes the integration cost of EVCI into PDN by attaining the most cost-effective ESS allocation and/or PDN reinforcement.

PEV charging demand at each facility is firstly estimated for inclusion in the PDN load demand. This estimation is based on the average number of busy chargers $E[\mathbb{B}_{t,n}]$ at time t in charging facility n, in addition to the charging power, P_n^{Ch}, and the charging efficiency, η_n^{Ch}, of chargers at facility n.[2] The calculation of $E[\mathbb{B}_{t,n}]$ can be done based on the analysis of the networked EVCI [33], as discussed in Subsection II-A. The power demand, $P_{t,n}^{EV}$, of charging facility n at time slot t can be computed by

$$E[\mathbb{B}_{t,n}] = \sum_{i=0}^{c_n} i p_{i_{t,n}} + c_n \sum_{i=c_n+1}^{K_n} p_{i_{t,n}} \tag{10a}$$

$$P_{t,n}^{EV} = \eta_n^{Ch} P_n^{Ch} E[\mathbb{B}_{t,n}]. \tag{10b}$$

To reduce the charging time, it is recommended that PEV users charge their PEV batteries to about 80% of capacity using constant current charging mode [6]. Based on this assumption and to simplify the calculations, P_n^{Ch} is regarded as constant [14], [32]. Although the charging power is assumed constant, the charging duration of each PEV is assumed to be an independently and exponentially distributed random variable, as discussed in Subsection II-A. This assumption conforms with the PEV battery charging behavior model and reflects the stochastic variability of PEV characteristics and users charging/driving behaviors [7]. After estimating the load demand of charging facilities, EVCI can be integrated into PDN, in which the objective function and constraint sets are described as follows.

A. OBJECTIVE FUNCTION

The objective function aims to minimize the total capital cost of EVCI integration into PDN, which includes two parts. The first one is the total investment cost, including the cost ESS

[2]To estimate the PEV load demand, each charging facility is assumed to contain a homogeneous type of chargers with the same charging power. Further study is needed to model charging facilities with multiple types of chargers at one location.

allocation in charging facilities, in addition to the cost of upgrading the PDN substation(s) and/or feeders. The ESS cost consists of three components [34]: 1) The ESS power cost C^P, which represents the cost of power electronics equipment such as inverters and rectifiers; 2) The ESS energy cost C^E, which is the cost of the storage elements such as the batteries; 3) The ESS annual operational cost C_l^O at year l. The total ESS operational cost is brought to the year of investment by aggregating the annual costs over the ESS lifetime L and multiplied by the present value factor, with annual interest rate $\mathcal{I}$. Let C^{Sb} and C^F denote the costs of substation expanding and feeder upgrade, respectively. The total investment cost can be expressed as

$$C^{Inv} = \sum_{\forall n \in N} \left\{ C^P P_n^R + C^E E_n^R + \sum_{l=1}^{L} \frac{C_l^O E_n^R}{(1+\mathcal{I})^{l-1}} \right\} + \sum_{\forall j \in \mathcal{H}} C^{Sb} G_j^R + \sum_{\forall ij \in \mathcal{L}} C^F \ell_{ij} S_{ij}^R. \tag{11}$$

The second part of the objective function is the present value of the system daily operational cost during the ESS lifetime. It includes 1) the cost of importing energy from the upstream grid, which is calculated based on the day-ahead hourly energy cost $C_{s,t}^e$ and the power injected to the system through the substation(s), and 2) the benefit from ESS energy arbitrage, which is the profit resulting from ESS charging during the off-peak periods at a low price and ESS discharging at the peak periods at a high price [3]. Let D_s denote the number of days in load scenario s in one year. Including the energy arbitrage in the objective function optimizes the ESS charging/discharging schedule. The total operational cost can be expressed as

$$C^{Opr} = \sum_{l=1}^{L} \frac{1}{(1+\mathcal{I})^{l-1}} \sum_{\forall s \in S} D_s \left\{ \sum_{\forall t \in T} \left\{ \sum_{\forall j \in \mathcal{H}} C_{s,t}^e P_{s,t,j}^G + \sum_{\forall n \in N} C_{s,t}^e P_{s,t,n}^{ES} \right\} \right\}. \tag{12}$$

B. ESS OPERATIONAL CONSTRAINTS

The following constraints regulate the ESS allocation and operation in charging facilities. These constraints should be satisfied for $\forall n \in N$, $\forall s \in S$, and $\forall t \in T$:

$$P_n^R = P^S p_n \le P_n^{R,\max} \tag{13a}$$

$$E_n^R = E^S e_n \le E_n^{R,\max} \tag{13b}$$

$$E_{s,t+1,n} = E_{s,t,n} + \eta^{ES} P_{s,t,n}^{ES} \Delta t \tag{13c}$$

$$E_{s,0,n} = E_{s,|T|,n} = E^{In} \tag{13d}$$

$$E^{\min} \le E_{s,t,n} \le E_n^R \tag{13e}$$

$$-P_n^R \le P_{s,t,n}^{ES} \le P_n^R. \tag{13f}$$

Constraints (13a) and (13b) determine the power rating and energy capacity of the allocated ESSs, respectively. Decision variables p_n (≥ 0) and e_n (≥ 0) are chosen to be integers because ESS components are usually available in discrete sizes (modules) [3], where P^S and E^S denote the available module steps for ESS power rating and energy capacity, respectively. The maximum rated power and energy of an ESS in charging facility n are limited to $P_n^{R,\max}$ and $E_n^{R,\max}$, respectively. Constraint (13c) models the state-of-charge (SoC) dynamics of an ESS at any time slot, where $\triangle t$ is time segment duration and η is the charging/discharging efficiency. Constraint (13d) represents the daily initial and final SoC requirements, where E^{In} denotes the daily initial SoC of an ESS. The operator can set the value of E^{In} based on the required reserve of power. This constraint links between consecutive days by ensuring that the stored energy at the end of each day is transferred to the next day [35], [36]. Constraint (13e) enforces the SoC upper and lower bound limitations, where $E^{\min}$ denotes the minimum SoC of an ESS. Constraint (13f) limits the injecting/extracting power into/from the ESS; positive power means that the ESS is charging, while negative power means that the ESS is discharging.

C. SYSTEM UPGRADE CONSTRAINTS

The following constraints regulate the substation(s) and feeders capacity upgrades.[3] These constraints should be satisfied for $\forall j \in \mathcal{H}$, $\forall ij \in \mathcal{L}$, $\forall s \in S$, and $\forall t \in T$:

$$G_j^R = G^S g_j \tag{14a}$$

$$S_{ij}^R = F^S f_{ij} \tag{14b}$$

$$0 \le P_{s,t,j}^G \le P_j^{G,\max} + G_j^R \tag{14c}$$

$$Q_j^{G,\min} \le Q_{s,t,j}^G \le Q_j^{G,\max} \tag{14d}$$

$$-\left(S_{ij}^{\max} + S_{ij}^R\right) \le P_{s,t,ij} \le \left(S_{ij}^{\max} + S_{ij}^R\right) \tag{14e}$$

$$-\left(S_{ij}^{\max} + S_{ij}^R\right) \le Q_{s,t,ij} \le \left(S_{ij}^{\max} + S_{ij}^R\right) \tag{14f}$$

$$-\sqrt{2}\left(S_{ij}^{\max} + S_{ij}^R\right) \le P_{s,t,ij} + Q_{s,t,ij} \le \sqrt{2}\left(S_{ij}^{\max} + S_{ij}^R\right) \tag{14g}$$

$$-\sqrt{2}\left(S_{ij}^{\max} + S_{ij}^R\right) \le P_{s,t,ij} - Q_{s,t,ij} \le \sqrt{2}\left(S_{ij}^{\max} + S_{ij}^R\right). \tag{14h}$$

Constraints (14a) and (14b) determine the required reinforcements of the substation(s) and feeders capacities. Decision variables $g_j(\ge 0)$ and $f_{ij}(\ge 0)$ are chosen to be integers because substation and feeder upgrade is assumed to be available in discrete steps, where G^S and F^S denote the available steps for substation and feeder upgrade, respectively. Constraints (14c) and (14d) limit the active and reactive power supplied by the substation(s), where $P_j^{G,\max}$, $Q_j^{G,\max}$, and $Q_j^{G,\min}$ denote the maximum active power, maximum reactive power,

[3]This model makes preliminary decisions on the substation(s) and feeder capacity upgrades. More detailed PDN expansion models that include various types of substation transformers and feeder conductors as well as accounting for any revised impedances resulting from upgrades can be found in [37], [38].

and minimum reactive power of existing substation connected to bus j, repectively. Constraints (14e)–(14h) represent the linearized branch power capacity limitations [39].

D. PDN OPERATIONAL CONSTRAINTS

A second order cone programming (SOCP) relaxation of the *DistFlow* model [40] is adopted in the power flow analysis of the balanced radial PDN. The following constraints should be satisfied for $\forall ij \in \mathcal{L}$, $\forall j \in \mathcal{B}$, $\forall s \in S$, and $\forall t \in T$:

$$P_{s,t,ij} = -P^{G}_{s,t,j} + P^{ES}_{s,t,n} + P^{EV}_{t,n} + P^{D}_{s,t,j} + r_{ij}L_{s,t,ij} + \sum_{m:j\to m} P_{s,t,jm}, \quad \text{if } n \to j \tag{15a}$$

$$Q_{s,t,ij} = -Q^{G}_{s,t,j} + Q^{D}_{s,t,j} + x_{ij}L_{s,t,ij} + \sum_{m:j\to m} Q_{s,t,jm} \tag{15b}$$

$$V_{s,t,i} - V_{s,t,j} = -\left(r^2_{ij} + x^2_{ij}\right) L_{s,t,ij} + 2(r_{ij}P_{s,t,ij} + x_{ij}Q_{s,t,ij}) \tag{15c}$$

$$L_{s,t,ij}V_{s,t,i} \geq P^2_{s,t,ij} + Q^2_{s,t,ij} \tag{15d}$$

$$(v_{\min})^2 \leq V_{s,t,i} \leq (v_{\max})^2. \tag{15e}$$

Constraints (15a) and (15b) represent real and reactive power balance at PDN branches, where $n \to j$ and $j \to m$ denote a direct line connection either between charging facility n and bus j or between bus j and another bus m, respectively. Branch resistance and reactance are denoted by r_{ij} and x_{ij}. Bus voltage and current flow constraints are introduced in (15c) and (15d), respectively. Finally, constraint (15e) enforces the upper and lower bounds on bus voltage magnitude.

Based on the preceding discussion, the integration problem is formulated as a mixed integer SOCP problem given by

$$\begin{aligned} \min_{\mathbf{p},\mathbf{e},\mathbf{g},\mathbf{f}} \quad & C^{Opr} + C^{Inv} \ (11)\text{–}(12) \\ \text{s.t.} \quad & \text{ESS operational constraints (13a)–(13f)} \\ & \text{System upgrade constraints (14a)–(14h)} \\ & \text{PDN operational constraints (15a)–(15e).} \end{aligned} \tag{16}$$

V. NUMERICAL RESULTS

The performance of the proposed capacity planning framework is evaluated in this section. We consider a small network of three charging facilities, and explore the key relationships among network characteristics. Throughout this case study, we use the Nguyen-Dupuis RTN, which is shown in Fig. 3(a), where the network attributes are given in [2]. The time-varying traffic volumes are simulated based on the dynamic traffic assignment model using the traffic simulator SUMO. The PDN under study is a 33-bus radial system, as shown in Fig. 3(b), where buses and branches data are given in [41]. The RTN nodes/links geographically overlap with the PDN buses, which means that each RTN node or link is served by one electric bus of PDN. In the integration with PDN model, we considered four typical daily load scenarios (winter, spring, fall, and summer), which follow the hourly load shape of the IEEE-RTS [42]. Moreover, the energy prices follow the hourly Ontario energy price provided by IESO for diffrent seasons [17]. Each RTN node or link is physically connected to a PDN bus. The sizing problem is solved by nonlinear black-box optimizer Knitro version 12. The EVCI integration into the PDN problem is solved by Gurobi Optimizer version 8.1. Both models are implemented in a Python 3.7 environment. The numerical results are obtained on a laptop computer with a 2.3-GHz Intel(R) Core(TM) i5-8300H CPU and 8 GB of memory.

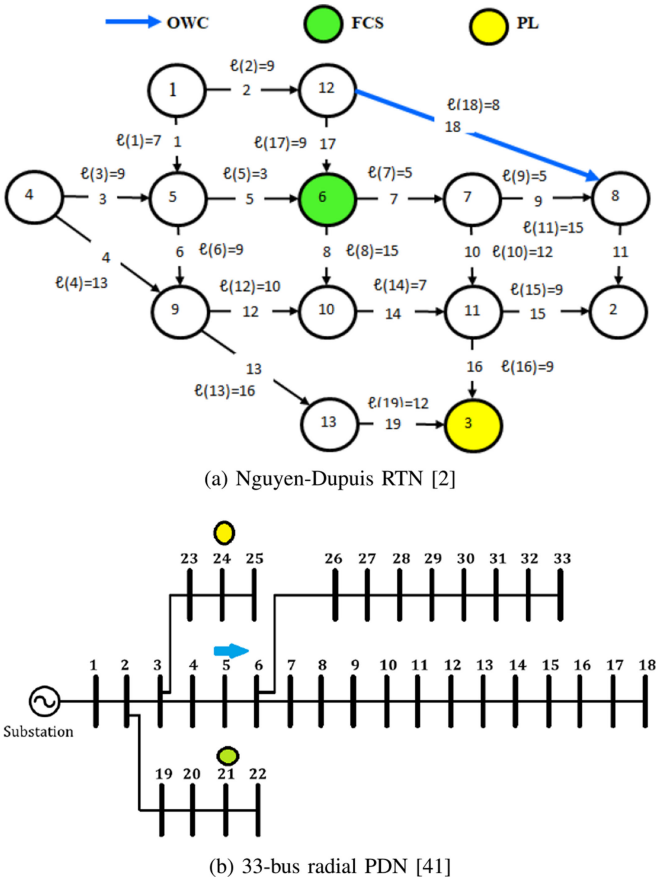

(a) Nguyen-Dupuis RTN [2]

(b) 33-bus radial PDN [41]

FIGURE 3. System under study.

We consider EVCI consists of three charging facilities allocated on the Nguyen-Dupuis RTN, which are FCS at node 6, OWC at link 18, and PL at node 3. In this case study, FCS, OWC, and PL are connected to PDN buses 21, 5 and 24, respectively. These charging facilities are serving 1500 PEVs uniformly distributed within origin-destination pairs of the RTN. DC level 2 chargers with 90 kW charging power are assigned in the FCS, and three-phase AC level 3 chargers with 43.5 kW are used in the PL [18]. The charging power of wireless chargers is not standardized yet; however, 22 kW wireless charging panels are assumed for the OWC [19]. Currently popular PEV models (e.g., Tesla Model S) have battery capacity 95 kWh. Such PEV can be fully charged using a DC fast charger in 38 minutes and a three-phase AC charger in 6 hours. PEV manufacturers recommend battery charging to about

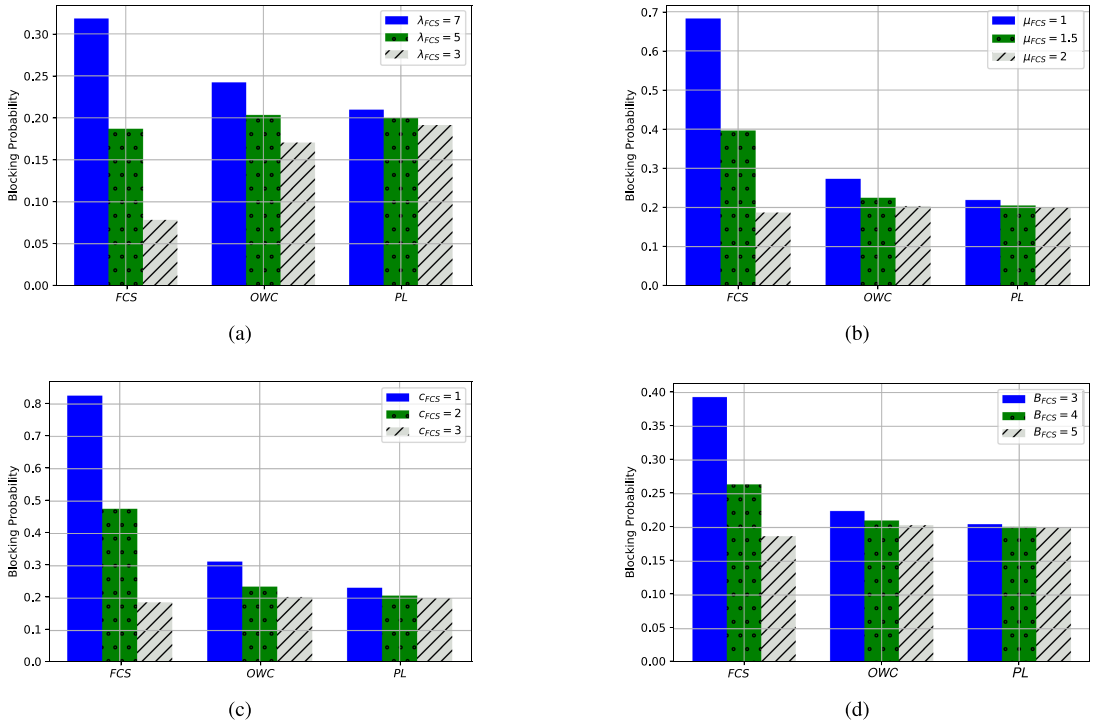

FIGURE 4. Assessment of EVCI blocking probabilities against the variation of FCS characteristics: (a) Arrival rate, (b) Service rate, (c) Number of chargers, (d) Number of waiting positions.

80% SoC to reduce charging time. Thus, the mean charging time is set to 30 minutes ($\mu^F = 2$) in FCSs, 10 minutes ($\mu^W = 6$) in OWC, and 3 hours ($\mu^P = 0.3$) in PLs. An open queuing network with finite capacity and RS-RD blocking is constructed as described in Subsection II-A. The state probabilities of the queuing network nodes are evaluated based on the DA algorithm. The routing probability between a DN and the associated CN is set at 0.6. The routing probability between any two facilities in the network is calculated based on (1).

We firstly examine the performance of the EVCI with stationary arrival rates to explore the relationships among network characteristics. Subsequently, we present the capacity planning of the charging network with more realistic time-varying arrival process and evaluate the time-varying performance metrics. It is shown that the capacity planning framework can achieve targeted performance metrics. Finally, we integrate the EVCI into the PDN, and investigate the relationship between the targeted QoS and the required investment in PDN.

A. PERFORMANCE WITH STATIONARY ARRIVALS

This experiment demonstrates the interplay between characteristics of a charging facility on the performance of the other facilities in the network. The blocking probabilities of the three charging facilities are inspected under the alteration of external arrival rate, service rate, number of chargers, and number of waiting positions of the FCS. Number of chargers and waiting positions are set at $\mathbf{c} = \{3, 2, 5\}$ and $\mathbf{B} = \{2, 0, 2\}$ for FCS, OWC, and PL, respectively. The arrival process at OWC and PL are stationary with rate $\lambda_{OWC} = 5$ PEV/h and $\lambda_{PL} = 3$ PEV/h, while the arrival rate at FCS is varied with $\lambda_{FCS} = \{7, 5, 3\}$ PEV/h. As shown in Fig. 4(a), increasing λ_{FCS} leads to a proportional increase in the blocking probabilities of the three facilities, and vice verse. It can be noted also that the variations are higher in the OWC statistics than the PL. This is because the routing probability towards OWC is higher than PL. A similar effect is observed if we alter the service rate, the number of chargers, and the number of waiting positions, as shown in Fig. 4(b), 4(c), and 4(d), respectively. This experiment shows that the performance of a charging facility in a network may be highly impacted by the characteristics of the neighboring charging facilities. Consequently, EVCI must be designed as a network to account for the inter-relationships among nearby facilities.

B. PERFORMANCE WITH TIME-VARYING ARRIVALS

We present the capacity planning of the networked EVCI with more realistic time-varying arrival rates. The objective of the experiment is to optimize the charging facility sizes to achieve the predetermined targeted performance metrics for the networked EVCI. These targets are set to be 90% minimum network throughput and 10 minutes maximum expected waiting time.

In order to solve this sizing problem, the MOL arrival rates are firstly estimated based on (4). The time-varying numbers of PEVs intercepted with charging facilities are extracted from traffic simulation. The statistical parameters used in arrival rate estimation are given and summarized in Table 1. The listed PEV population parameters are used for illustration purposes. In practice, the system planner should adopt the

TABLE 1. Parameters Settings

Parameter	Value	Parameter	Value
ν	0.65 [11]	η^{Ch}	90% [18]
μ^F	2 PEV/h [2]	σ	30%
μ^W	6 PEV/h [2]	β	40%
μ^P	0.3 PEV/h [2]	L	5 years [35]
C^P	175 $/kW [3]	$\mathcal{I}$	1% [3]
C^E	305 $/kWh [3]	η^{ES}	95% [43]
C^O_y	15 $/kWh/year [3]	E^{In}	50% [43]
C^{Sb}	788 $/kVA [6]	$E^{\min}$	10% [43]
C^F	120 $/kVA.km [6]	$v_{\min}/v_{\max}$	0.9/1.1 p.u. [10]

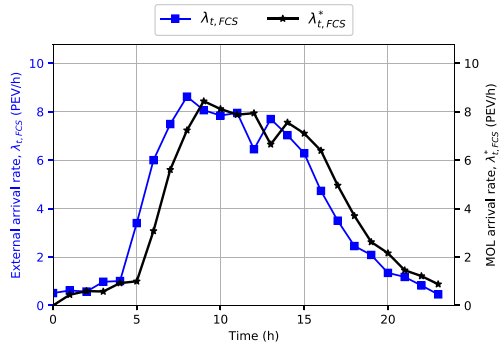

(a) FCS

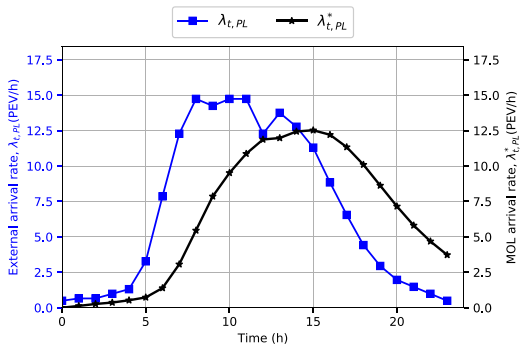

(b) PL

FIGURE 5. External arrival rate versus MOL arrival rate.

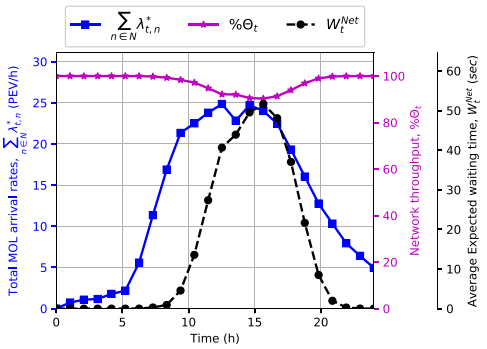

(a) EVCI network

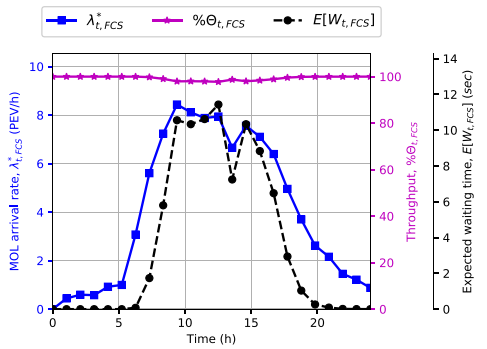

(b) FCS

FIGURE 6. Time-varying performance of the EVCI.

actual PEV statistical parameters, which can be collected from market surveys.

Fig. 5 shows the external arrival rate and the MOL arrival rate of both FCS and PL as a function of the time slot index. It can be noted that there are a magnitude difference and a phase shift between λ_t and λ^*_t, which account for time-lag and magnitude difference between the external arrivals and the system loads. This difference is significantly increased as the service time of the facility increases, as shown in Fig. 5(b). The MOL arrival rate functions are used to analyze the non-stationary queuing models.

The sizing problem, in (9), minimizes the total numbers of chargers and waiting positions allocated in charging facilities to achieve the targeted network throughput and average waiting time. Both chargers and waiting positions are assumed to have a similar cost $\omega_n = 0.5, \forall n \in N$. The objective function has a minimal value at $\mathbf{c} = \{7, 4, 22\}$ and $\mathbf{B} = \{1, 0, 2\}$. Fig. 6(a) shows the time-varying performance metrics of the networked EVCI. It is observed that $\underline{\Theta} = 90.13\%$ and $\overline{W^{Net}} = 51.6$ seconds, which achieve the predetermined QoS targets. A similar trend can be observed in the performance of the individual charging facilities, as shown in Fig. 6(b).

Substantial differences appear when comparing the results of the proposed sizing approach with those of sizing models based on the isolated stationary queuing employed in [2], [8]. Based on the $M/M/c/K$ queuing model, the numbers of allocated chargers and waiting positions in the EVCI are $\mathbf{c} = \{3, 1, 21\}$ and $\mathbf{B} = \{1, 0, 1\}$, respectively. Note that the numbers of the allocated chargers and waiting positions based on the isolated stationary queuing model are less than those using our proposed approach. This is because the isolated queuing models do not account for the propagation of congestion due to the behaviors of the blocked PEV users. Also, stationary queuing models determine the charging facility size based on the daily peak demand without considering the PEVs that are already in the facility from the preceding time periods.

The computational time of the sizing problem is highly dependent on the number of charging facilities in the network. For instance, the solution time for the EVCI under investigation is 19 hours. However, the solution time for a network of two charging facilities is around 1 hour. Since the sizing problem should be solved offline in the system planning stage, the computation complexity should not pose a significant challenge.

TABLE 2. Detailed Integration Plans for the EVCI Network With the PDN

QoS target		60%	70%	80%	90%
Total capital cost		$\$3.77\times10^6$	$\$4.17\times10^6$	$\$4.24\times10^6$	$\$4.33\times10^6$
Substation	Upgrade	0	0.5 MVA	0.5 MVA	0.5 MVA
	Cost	0	\$394,000	\$394,000	\$394,000
Feeders	Upgrade	0	(0,1): 0.5 MVA	(0,1): 0.5 MVA	(0,1): 0.5 MVA
	Cost	0	\$60,000	\$60,000	\$60,000
ESS	Allocated	(0.2 MW, 0.5 MWh) (0.1 MW, 0.1 MWh)	0	(0.1 MW, 0.1 MWh)	(0.1 MW, 0.1 MWh) (0.1 MW, 0.2 MWh)
	Cost	\$279,618	0	\$55,353	\$148,559
Energy cost		$\$3.53\times10^6$	$\$3.72\times10^6$	$\$3.74\times10^6$	$\$3.75\times10^6$
Arbitrage profit		\$36,061	0	\$9,066	\$23,416

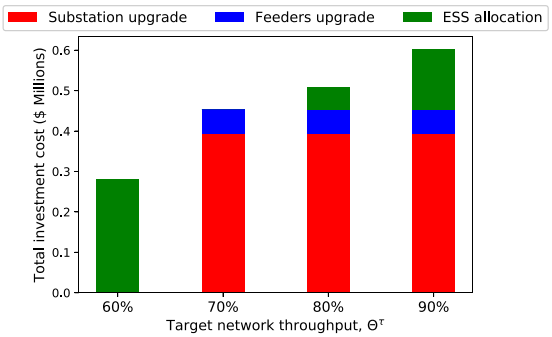

FIGURE 7. QoS targets versus the required PDN investment.

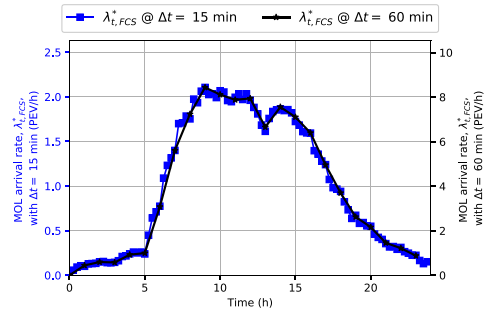

(a) MOL arrival rate

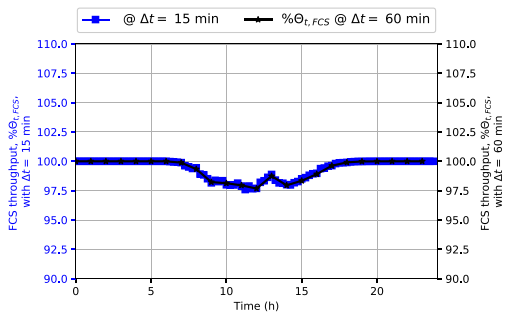

(b) FCS throughput

FIGURE 8. EVCI performance with different time intervals.

C. INTEGRATION INTO PDN

In integrating the EVCI network with the PDN, we aim to investigate the relationship between the targeted QoS level and the required investment in the PDN. The proposed integration model minimizes the total investment and operation cost by allocating ESS in charging facilities and/or upgrading the PDN substation and feeders. The substation capacity is 5 MVA, and the system peak load demand is 3.715 MW (without EVCI loads). The ESSs are available in discrete power and energy capacities with step size of 100 kW and 100 kWh, respectively. The reinforcement of the substation and feeders are available with step size of 250 kVA. Other financial and technical parameters are summarized in Table 1.

We analyze the effect of varying network throughput target on the investment cost of the EVCI network integration into the PDN. Fig. 7 illustrates the total investment cost for each QoS target, and the detailed integration plans are shown in Table 2. When the targeted network throughput is set to 60%, ESSs are allocated in the EVCI. On the other hand, when the QoS target is set to 70%, upgrading the PDN substation and feeders is a more cost-efficient solution. In the case of $\Theta^\tau = 60\%$, it can be noted that the allocated ESS is higher than the other cases. This is because ESS capacities, as well as feeders and substation reinforcement, are assumed available in discrete steps. Then, the proposed model chooses the lowest cost combination of the allocated ESS and PDN reinforcement to minimize the total capital cost. Hence, in the case of a 60% throughput target, it is cheaper to allocate ESSs than upgrade the feeders and substation. The solution time for the integration into PDN problem under investigation is 8 minutes. Consequently, the required investment in the PDN is highly dependent on the capability of the existing PDN components and the targeted QoS of the EVCI. Also, allocating ESSs in charging facilities can be a cost-effective solution to alleviate the required PDN upgrades if ESS cost is less than the reinforcement cost.

D. SENSITIVITY ANALYSIS

1) IMPACT OF TIME SEGMENT DURATION

Time segment duration (i.e., $\triangle t$) effect is investigated with $\triangle t = 15$ min and compared with the results with $\triangle t = 1$ hour. As shown in Fig. 8(a), using the shorter time interval scales down the MOL arrival rate at charging facilities. However, the observed EVCI performance is similar for both cases, as shown in Fig. 8(b). This is because the proposed approach utilizes the nonstationary queuing models, which account for PEVs that are already in the system (either charging or waiting) from the preceding time periods.

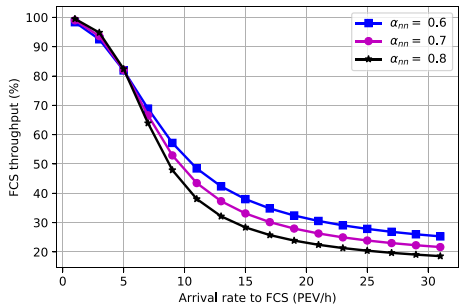

FIGURE 9. FCS throughput versus arrival rate with various routing probabilities.

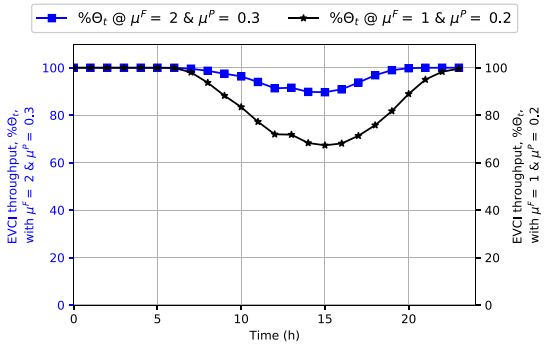

FIGURE 10. Influence of mean charging time on EVCI throughput.

2) IMPACT OF THE ROUTING PROBABILITY VALUE BETWEEN A DN AND THE ASSOCIATED CN

A slight shift in the performance occurs at the overloaded charging facility with an increase of the routing probability value between a DN and the associated CN (i.e., α_{nn}), as shown in Fig. 9. This is because, in the networked EVCI model, only a small percentage of the blocked PEVs are choosing the same charging facility instead of routing to another facility. In practice, a PEV user will choose another facility after being blocked at one facility. Since this shift in the performance is observed only at the overloaded charging facilities, it may not affect the capacity planning problem with acceptable QoS targets.

3) IMPACT OF THE VARIATIONS OF THE MEAN CHARGING TIME

We have examined the EVCI performance with different PEV charging power capability. For instance, if most of the PEVs in the system can only charge with 50 kW DC fast chargers at FCS and 7.4 kW AC level 2 chargers at PL, the PEV charging time at these facilities increases. In this case, for the commonly available PEVs with 60–70 kWh battery capacity, the service time is 1 hour ($\mu^F = 1$) in FCS and 5 hours ($\mu^P = 0.2$) in PL [44]. As shown in Fig. 10, the EVCI throughput decreases with the increasing of the mean service time, as charging facilities will be occupied for a longer time. Thereby, the capacity planning of EVCI must account for the charging characteristic of PEVs in the system to achieve the targeted performance.

VI. CONCLUSION

In this paper, we study capacity planning of EVCI and propose a framework that sizes charging facilities to fulfill the given QoS targets. The proposed framework minimizes the cost of EVCI integration into PDN by either allocating ESSs in charging facilities and/or reinforcing the PDN. The link between the targeted QoS level and the PDN capability offers insights into how to make a trade-off between the PEV user satisfaction and the required investment in PDN. Our framework captures the correlation among the occupancy of neighboring charging facilities, which ensures that the targeted QoS level is achieved for the entire networked EVCI. Furthermore, the proposed framework accounts for the temporal variability of PEV charging demand by addressing the time-lag and magnitude shift between arrivals and loads of the system. The numerical results demonstrates that the inter-relationship between the targeted QoS level and the required investment in the PDN plays a vital role in capacity planning of EVCI. The proposed framework can be extended by optimizing the QoS target to maximize user satisfaction within a budget limit. In this case, both the EVCI capacity planning model and integration with the PDN model can be simultaneously solved. This extension is to address the trade-off between the targeted QoS level of EVCI and the required investment in both EVCI and PDN.

REFERENCES

[1] A. Abdalrahman and W. Zhuang, "A survey on PEV charging infrastructure: Impact assessment and planning," *Energies*, vol. 10, no. 10, pp. 1650–1674, 2017.
[2] A. Abdalrahman and W. Zhuang, "PEV charging infrastructure siting based on spatial-temporal traffic flow distribution," *IEEE Trans. Smart Grid*, vol. 10, no. 6, pp. 6115–6125, Nov. 2019.
[3] A. S. Awad, T. H. EL-Fouly, and M. M. Salama, "Optimal ESS allocation for benefit maximization in distribution networks," *IEEE Trans. Smart Grid*, vol. 8, no. 4, pp. 1668–1678, Jul. 2017.
[4] C. Kong, R. Jovanovic, I. S. Bayram, and M. Devetsikiotis, "A hierarchical optimization model for a network of electric vehicle charging stations," *Energies*, vol. 10, no. 5, pp. 675–694, 2017.
[5] S. Bae and A. Kwasinski, "Spatial and temporal model of electric vehicle charging demand," *IEEE Trans. Smart Grid*, vol. 3, no. 1, pp. 394–403, Mar. 2012.
[6] H. Zhang, S. J. Moura, Z. Hu, and Y. Song, "PEV fast-charging station siting and sizing on coupled transportation and power networks," *IEEE Trans. Smart Grid*, vol. 9, no. 4, pp. 2595–2605, Jul. 2018.
[7] O. Hafez and K. Bhattacharya, "Queuing analysis based PEV load modeling considering battery charging behavior and their impact on distribution system operation," *IEEE Trans. Smart Grid*, vol. 9, no. 1, pp. 261–273, Jan. 2018.
[8] M. Ismail, I. S. Bayram, M. Abdallah, E. Serpedin, and K. Qaraqe, "Optimal planning of fast PEV charging facilities," in *Proc. IEEE First Workshop Smart Grid Renewable Energy*, 2015, pp. 1–6.
[9] I. S. Bayram, G. Michailidis, M. Devetsikiotis, and F. Granelli, "Electric power allocation in a network of fast charging stations," *IEEE J. Sel. Areas Commun.*, vol. 31, no. 7, pp. 1235–1246, Jul. 2013.
[10] M. F. Shaaban, S. Mohamed, M. Ismail, K. Qaraqe, and E. Serpedin, "Joint planning of smart EV charging stations and DGs in eco-friendly remote hybrid microgrids," *IEEE Trans. Smart Grid*, vol. 10, no. 5, pp. 5819–5830, Sep. 2019.

[11] Y. Xiang, J. Liu, R. Li, F. Li, C. Gu, and S. Tang, "Economic planning of electric vehicle charging stations considering traffic constraints and load profile templates," *Appl. Energ.*, vol. 178, pp. 647–659, 2016.
[12] W. Yao *et al.*, "A multi-objective collaborative planning strategy for integrated power distribution and electric vehicle charging systems," *IEEE Trans. Power Syst.*, vol. 29, no. 4, pp. 1811–1821, Jul. 2014.
[13] G. Wang, Z. Xu, F. Wen, and K. P. Wong, "Traffic-constrained multi-objective planning of electric-vehicle charging stations," *IEEE Trans. Power Del.*, vol. 28, no. 4, pp. 2363–2372, Oct. 2013.
[14] Z. Sun, X. Zhou, J. Du, and X. Liu, "When traffic flow meets power flow: On charging station deployment with budget constraints," *IEEE Trans. Veh. Technol.*, vol. 66, no. 4, pp. 2915–2926, Apr. 2017.
[15] H. Zhang, S. J. Moura, Z. Hu, W. Qi, and Y. Song, "A second-order cone programming model for planning PEV fast-charging stations," *IEEE Trans. Power Syst.*, vol. 33, no. 3, pp. 2763–2777, May 2018.
[16] J. A. Schwarz, G. Selinka, and R. Stolletz, "Performance analysis of time-dependent queueing systems: Survey and classification," *Omega*, vol. 63, pp. 170–189, 2016.
[17] Independent Electricity System Operator (IESO), "Hourly Ontario Energy Price (HOEP)," 2019. [Online]. Available: http://www.ieso.ca/Power-Data/Price-Overview/Hourly-Ontario-Energy-Price, Accessed: May 14, 2019.
[18] A. Khaligh and M. D'Antonio, "Global trends in high-power on-board chargers for electric vehicles," *IEEE Trans. Veh. Technol.*, vol. 68, no. 4, pp. 3306–3324, Apr. 2019.
[19] S. Y. Choi, S. Y. Jeong, B. W. Gu, G. C. Lim, and C. T. Rim, "Ultraslim S-type power supply rails for roadway-powered electric vehicles," *IEEE Trans. Power Electron.*, vol. 30, no. 11, pp. 6456–6468, Nov. 2015.
[20] N. Wisitpongphan, F. Bai, P. Mudalige, V. Sadekar, and O. Tonguz, "Routing in sparse vehicular ad hoc wireless networks," *IEEE J. Sel. Areas Commun.*, vol. 25, no. 8, pp. 1538–1556, Oct. 2007.
[21] S. Balsamo, "Queueing networks with blocking: Analysis, solution algorithms and properties," in *Network Performance Engineering*. Berlin, Germany: Springer, 2011, pp. 233–257.
[22] S. Balsamo, V. D. N. Personè, and P. Inverardi, "A review on queueing network models with finite capacity queues for software architectures performance prediction," *Perform. Eval.*, vol. 51, no. 2–4, pp. 269–288, 2003.
[23] G. H. Mohimani, F. Ashtiani, A. Javanmard, and M. Hamdi, "Mobility modeling, spatial traffic distribution, and probability of connectivity for sparse and dense vehicular ad hoc networks," *IEEE Trans. Veh. Technol.*, vol. 58, no. 4, pp. 1998–2007, May 2008.
[24] M. C. Bliemer and P. H. Bovy, "Impact of route choice set on route choice probabilities," *Transp. Res. Rec.*, vol. 2076, no. 1, pp. 10–19, 2008.
[25] J. C. Strelen, B. Bärk, J. Becker, and V. Jonas, "Analysis of queueing networks with blocking using a new aggregation technique," *Ann. Oper. Res.*, vol. 79, pp. 121–142, 1998.
[26] L. M. Leemis, "Nonparametric estimation and variate generation for a nonhomogeneous Poisson process from event count data," *IIE Trans.*, vol. 36, no. 12, pp. 1155–1160, 2004.
[27] Z. Feldman, A. Mandelbaum, W. A. Massey, and W. Whitt, "Staffing of time-varying queues to achieve time-stable performance," *Manage. Sci.*, vol. 54, no. 2, pp. 324–338, 2008.
[28] L. V. Green, P. J. Kolesar, and W. Whitt, "Coping with time-varying demand when setting staffing requirements for a service system," *Prod. Oper. Manage.*, vol. 16, no. 1, pp. 13–39, 2007.
[29] T. Van Woensel, R. Andriansyah, F. R. Cruz, J. M. Smith, and L. Kerbache, "Buffer and server allocation in general multi-server queueing networks," *Int. Trans. Oper. Res.*, vol. 17, no. 2, pp. 257–286, 2010.
[30] O. Exler and K. Schittkowski, "A trust region SQP algorithm for mixed-integer nonlinear programming," *Optim. Lett.*, vol. 1, no. 3, pp. 269–280, 2007.
[31] R. H. Byrd, J. Nocedal, and R. A. Waltz, "KNITRO: An integrated package for nonlinear optimization," in *Large-Scale Nonlinear Optimization*. Berlin, Germany: Springer, 2006, pp. 35–59.
[32] J. Y. Yong, V. K. Ramachandaramurthy, K. M. Tan, and N. Mithulananthan, "A review on the state-of-the-art technologies of electric vehicle, its impacts and prospects," *Renew. Sust. Energy Rev.*, vol. 49, pp. 365–385, 2015.
[33] P. Köchel, "Finite queueing systems: Structural investigations and optimal design," *Int. J. Prod. Econ.*, vol. 88, no. 2, pp. 157–171, 2004.
[34] P. Poonpun and W. T. Jewell, "Analysis of the cost per kilowatt hour to store electricity," *IEEE Trans. Energy Convers.*, vol. 23, no. 2, pp. 529–534, Jun. 2008.
[35] H. Xing, H. Cheng, Y. Zhang, and P. Zeng, "Active distribution network expansion planning integrating dispersed energy storage systems," *IET Gener. Transmiss. Distrib.*, vol. 10, no. 3, pp. 638–644, 2016.
[36] X. Shen, M. Shahidehpour, Y. Han, S. Zhu, and J. Zheng, "Expansion planning of active distribution networks with centralized and distributed energy storage systems," *IEEE Trans. Sustain. Energy*, vol. 8, no. 1, pp. 126–134, Jan. 2017.
[37] S. Wong, K. Bhattacharya, and J. Fuller, "Electric power distribution system design and planning in a deregulated environment," *IET Gener. Transmiss. Distrib.*, vol. 3, no. 12, pp. 1061–1078, 2009.
[38] P. M. de Quevedo, G. Muñoz-Delgado, and J. Contreras, "Impact of electric vehicles on the expansion planning of distribution systems considering renewable energy, storage, and charging stations," *IEEE Trans. Smart Grid*, vol. 10, no. 1, pp. 794–804, Jan. 2017.
[39] X. Chen, W. Wu, and B. Zhang, "Robust restoration method for active distribution networks," *IEEE Trans. Power Syst.*, vol. 31, no. 5, pp. 4005–4015, Sep. 2016.
[40] D. K. Molzahn *et al.*, "A survey of distributed optimization and control algorithms for electric power systems," *IEEE Trans. Smart Grid*, vol. 8, no. 6, pp. 2941–2962, Nov. 2017.
[41] M. E. Baran and F. F. Wu, "Network reconfiguration in distribution systems for loss reduction and load balancing," *IEEE Trans. Power Del.*, vol. 4, no. 2, pp. 1401–1407, Apr. 1989.
[42] C. Grigg, "The IEEE reliability test system-1996. A report prepared by the reliability test system task force of the application of probability methods subcommittee," *IEEE Trans. Power Syst.*, vol. 14, no. 3, pp. 1010–1020, Aug. 1999.
[43] S. Yao, P. Wang, and T. Zhao, "Transportable energy storage for more resilient distribution systems with multiple microgrids," *IEEE Trans. Smart Grid*, vol. 10, no. 3, pp. 3331–3341, May 2019.
[44] "Global EV outlook 2019, scaling-up the transition to electric mobility," The International Energy Agency (IEA), Paris, France, 2019.

AHMED ABDALRAHMAN received the B.Sc. degree with first class honors from the Thebes Higher Institute of Engineering, Cairo, Egypt, in 2008 and the M.Sc. degree from Ain Shams University, Cairo, Egypt, in 2013, both in electrical engineering. He is currently working toward the Ph.D. degree with the Department of Electrical and Computer Engineering, University of Waterloo, Waterloo, ON, Canada, where he is currently a Research Assistant. His current research interests include smart grids, optimization, and artificial intelligence.

He was the recipient of the 2020 Jon W. Mark Graduate Scholarship in Communication, and a recipient of several Faculty of Engineers Awards from the University of Waterloo. Beyond his academic contributions, he is an active member of several professional societies. He is an IEEE volunteer in various positions in Kitchener-Waterloo Section, Canada.

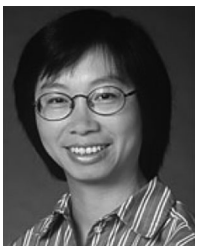

WEIHUA ZHUANG (Fellow, IEEE), since 1993, has been with the Department of Electrical and Computer Engineering, University of Waterloo, Waterloo, ON, Canada, where she is currently a Professor and a Tier I Canada Research Chair in Wireless Communication Networks.

She was the recipient of the 2017 Technical Recognition Award from the IEEE Communications Society Ad Hoc and Sensor Networks Technical Committee, and a corecipient of several Best Paper Awards from IEEE conferences. She was the Editor-in-Chief of the IEEE TRANSACTIONS ON VEHICULAR TECHNOLOGY from 2007 to 2013, the Technical Program Chair/Co-Chair of IEEE VTC 2017 Fall and 2016 Fall, and the Technical Program Symposia Chair of IEEE Globecom 2011. She is an elected member of the Board of Governors and the Vice-President - Publications of the IEEE Vehicular Technology Society. She was an IEEE Communications Society Distinguished Lecturer from 2008 to 2011. She is a Fellow of the Royal Society of Canada, the Canadian Academy of Engineering, and the Engineering Institute of Canada.